İmalat Teknolojileri ve Uygulamaları
Cilt: 4, No: 1, 2023 (49-58)
Araştırma Makalesi
e-ISSN: 2717-7475

Manufacturing Technologies and Applications
Vol: 4, Issue: 1, 2023 (49-58)
Research Article
e-ISSN: 2717-7475

Investigation of The Effect of Reduced Shank Thickness of Friction Welded Yoke Shaft on Strength

Onur ŞEN [1], Mert Can KAHYALAR[1]

[1]*Tirsan Kardan A.Ş., Ar-Ge Merkezi, Manisa, Turkey*

ARTICLE INFORMATION

Received: *29.03.2023*
Accepted: *27.04.2023*

Keywords:
Rotary friction welding
Yoke shaft
Wall thickness
FEA

ABSTRACT

Usage of friction welding method on the joints provides many advantages such as cost reduction, weight reduction and higher quality. The yoke shaft produced by rotary friction welding (RFW) involves a yoked part and a hollow round bar which are welded to each other. And so, no additional drilling method used in the way of removing material from the centre of the yoke shaft, is required to reduce the weight. The weight is inherently reduced thanks to hollow round bar used in RFW method. It is possible to use a friction welded yoke shaft in a wide range of wall thickness by removing material from the shank diameter for different applications. At this point, the key factor is strength of the friction welded yoke shaft with reduced wall thickness on the shank diameter. The aim of this study is investigation the effect of the reduced wall thickness of a yoke shaft produced by RFW on the strength. For this purpose, yoke shafts were manufactured by using RFW and consecutive processes such as turning and millings to reduce the wall thickness. The specimens in different wall thickness were tested to determine the strength. Additionally finite element analyses (FEAs) were implemented for each variation of the specimens and compared with the test results. As a result, it was determined that yoke shafts with reduced wall thicknesses, which were produced by RFW and then consecutively machining operations to obtain a specific wall thickness, can be used in drive shaft manufacturing securely.

Sürtünme Kaynaklı Çatallı Milin Boğaz Cidar Kalınlığındaki Azaltmanın Dayanım Üzerindeki Etkisinin İncelenmesi

MAKALE BİLGİSİ

Alınma: *29.03.2023*
Kabul: *27.04.2023*

Anahtar Kelimeler:
Dönel sürtünme kaynağı
Çatallı Mil
Cidar kalınlığı
FEA

ÖZET

Sürtünme kaynağı yönteminin birleştirmelerde kullanılması, maliyet düşürme, ağırlık azaltma ve daha yüksek kalite gibi birçok avantaj sağlar. Dönel sürtünme kaynağı (RFW) ile üretilen çatallı mil birbirine kaynaklanmış çatallı bir parça ve içi boş yuvarlak çubuk içerir. Ve bu nedenle, ağırlığı azaltmak için çatallı milin merkezinden malzeme azaltmak için kullanılan ek bir delme yöntemi gerekmez. RFW yönteminde kullanılan içi boş yuvarlak çubuk sayesinde ağırlık kendiliğinden azaltılmıştır. Farklı uygulamalar için boğaz çapından malzeme kaldırılarak çok çeşitli cidar kalınlıklarında sürtünme kaynaklı çatallı mil kullanmak mümkündür. Bu noktada kilit faktör, boğaz çapında azaltılmış cidar kalınlığına sahip sürtünme kaynaklı çatallı milin dayanımıdır. Bu çalışmanın amacı, RFW ile üretilen çatallı milin azaltılmış cidar kalınlığının parçanın dayanımı üzerindeki etkisinin araştırılmasıdır. Bu amaçla, RFW ve cidar kalınlığını azaltmak için tornalama ve frezeleme gibi ardışık işlemler kullanılarak çatallı miller üretilmiştir. Dayanımı belirlemek için farklı cidar kalınlıklarındaki numuneler test edilmiştir. Ek olarak, numunelerin her varyasyonu için sonlu eleman analizleri (FEA) uygulanmış ve test sonuçlarıyla karşılaştırılmıştır. Sonuç olarak RFW ve ardından belirli bir cidar kalınlığı elde etmek için ardışık talaşlı imalat işlemleri ile üretilen azaltılmış cidar kalınlığına sahip çatallı millerin kardan mili imalatında güvenle kullanılabileceği belirlenmiştir.

** Corresponding author, E-mail: senonurmail@gmail.com*
To cite this article: *Şen, Kahyalar, Investigation of The Effect of Reduced Shank Thickness of Friction Welded Yoke Shaft on Strength, Manufacturing Technologies and Applications 4(1), 49-58, 2023.*
https://doi.org/10.52795/mateca.1272866

1. INTRODUCTION (GİRİŞ)

Friction welding technique has become one of the major joining methods with its rising usage ratio in various industries such as automotive and aerospace where high-quality joints are needed. Difficulty of the joining of special materials used in automotive and aerospace requires using friction welding methods such as friction stir welding (FSW), linear friction welding (LFW) and rotary friction welding (RFW) [1]. Ferrous and non-ferrous alloys of various geometrical shapes can be joined with the same or different alloys by friction welding methods. Basically, friction welding method is a solid-state joining process in which heat is emerged during transformation of mechanical energy to thermal energy at the faying surface of the workpiece couple due to the rotation under exerted pressure. As a result of the said process, a metallic bonding is generated at lower temperatures compared to the melting point of the base material. Parameters effecting the friction and forging, and rotation speed are dominant on the product quality [2].

It is possible to handle FW in three ways depending on the relative movement of the workpieces: rotary, linear and orbital (Fig. 1). Rotary friction welding (RFW) is the most common type of friction welding in industry. In this method, one of the workpieces rotates about its axis while the other workpiece is stationary, and the workpieces are joined to each other under a friction pressure. RFW can be addressed in two different types in which rotation converted to friction heat is determinant: direct drive also known as continuous drive (CDFW) and inertia drive (IDFW) in which the energy is stored [3-5].

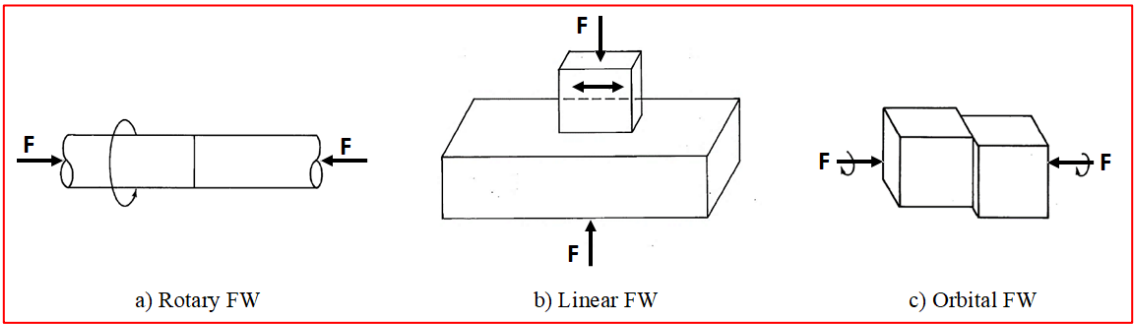

Figure 1. Relative movements of the workpieces in friction welding [6].

CDFW, which is the subject of the paper, is an extensively used friction welding method from the 1940's to the present. In this process whose steps and their relationships are illustrated in Fig. 2, one of the workpieces is stationary under an axial pressure while the other rotates at a constant speed [5-11]. Each workpiece contacts to each other and comes closer by axial pressure during a certain friction time. Right after, rotating workpiece is stopped within the braking time and the pressure on the stationary part is increased in a predetermined upset time. During the welding process, the narrow regions near the welding interface are rapidly heated by friction until they exhibit a steady state of high strain rate plastic flow. The welding process is then terminated with a forging stage to reinforce the joint [11,12]. Although CDFW has been experimentally proven to be a rapid and reliable method for joining the material pair which can be similar and dissimilar materials [13-17], a simple and accurate analytical thermo-mechanical model is still required to better understand heat generation and material flow during the process [11,18,19].

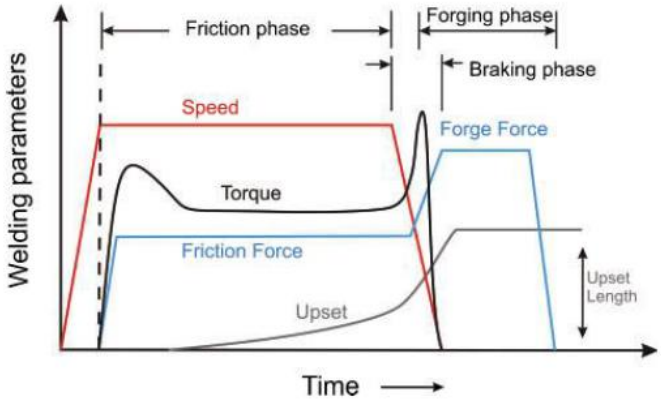

Figure 2. Critical welding parameters and their relationship for direct drive friction welding process [5].

When the literature is reviewed, it has been seen that the joining of the different materials together was the common subject handled in most of the studies. These studies addresses that the challenges encountered during the joining of dissimilar materials by friction welding, process parameters and mechanical properties of the final product as well. Some of the studies are about 6063 aluminum alloy and AISI 304 austenitic stainless-steel by Kimura at al. [20], YSZ–alumina composite and 6061 aluminium alloy by Uday et al. [21], AA1050 aluminum with AISI 304 stainless steel by Alves [22].

On the other hand, analytical models and literature review are the other main idea of the rest of the studies in literature. In one of these studies implemented by Xiong et al. [23], it was focused on an analytical model for continuous drive friction welding (CDFW). The results from analytical model and experiments were compared considering plastic region thickness, welding power, and average temperature. As a results, it was indicated that the analytical model could provide reliable descriptions during steady state CDFW. Maalekian [5] reviewed and investigated the literature.

Unlike these studies, this study handles the effect of the reduced shank thickness of friction welded yoke shaft on strength. In this context, different shank thicknesses were considered and examined with FEA software and tests under laboratory conditions.

2. MATERIAL AND METHOD (MATERYAL VE YÖNTEM)

The study basically includes two verification methods, finite element analyses (FEAs) and laboratory tests also known as bench test. Finite element analyses (FEAs) were applied on 3D data of yoke shaft specimens while the laboratory tests conducted with drive shaft specimens which are prepared for evaluation of the yoke shaft specimens.

The yoke shaft specimens were produced by respectively forging, implementing CDFW and machining processes applied as a finish operation. Following specimen production of yoke shafts, the specimens were examined for checking welding quality by using various inspection methods. Finally, drive shaft specimens were produced for laboratory tests conducted to check the performance of the yoke shaft with various wall thickness.

2.1. Specimen Preparation (Numune Hazırlama)

The production of the sub-components to be welded each other, which compose the welded yoke shaft, is the first step of the specimen production of yoke shaft. In this context, tube yokes with chemical composition defined in Table 1 were produced by the processes respectively close die hot forging, heat treatment and machining. Beside tube yokes, hollow round bars were prepared for FW by cutting and machining processes on the raw material with chemical composition defined in Table 1. The sub-components (tube yoke and hollow round bar) and welded yoke shaft were given in Figure 3.

Table 1. Chemical composition of sub-components in %mass: tube yoke and hollow round bar

	C	Si	Mn	P	S	Cr	Mo
Tube yoke	0.38-0.45	0.10-0.40	0.60-0.90	max 0.025	max 0.035	0.90-1.20	0.15-0.30
Hollow round bar	0.38-0.45	max 0.40	0.60-0.90	max 0.035	max 0.035	0.90-1.20	0.15-0.30

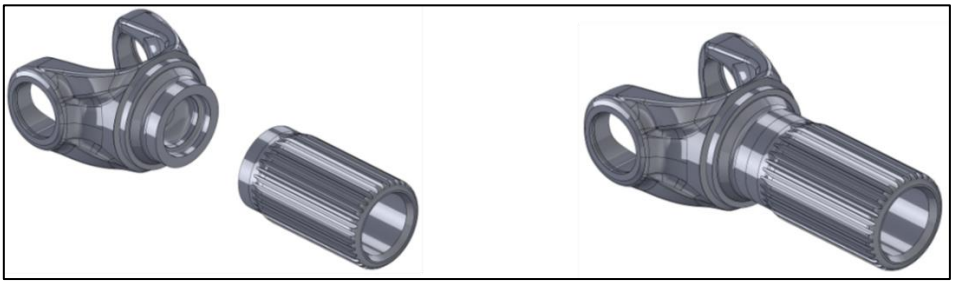

Figure 3. 3D data of tube yokes, hollow round bar and welded yoke shaft (Çatal, içi boş yuvarlak çubuk ve kaynaklı çatallı milin 3B verileri)

Sub-components were joined together by CDFW method as given in Figure 4. The picture of welded yoke shaft before and after finish operations, which are such as splining, turning, etc., was given by the Figure 5.

Figure 4. The yoke shaft during CDFW operation (CDFW işlemi sırasında çatallı mil)

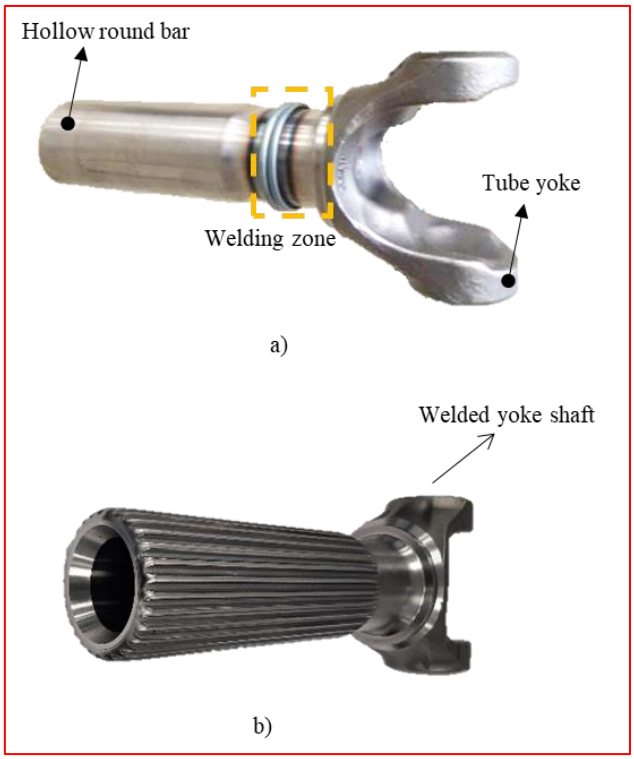

Figure 5. A welded yoke shaft specimen, a) before finish operations (splining, turning, etc.), b) after finish operations (splining, machining, etc.)

Mechanical and metallurgical properties of specimens were evaluated for checking the weld performance. And so, following testes and analyses were respectively performed on the weld cross-section for each of the specimens in different wall thickness.

- Hardness scan
- Bending test
- Macroscopic/microscopic inspection

Hardness scan

The main purpose of the hardness scan is to determine the distribution of hardness, and evaluation. A specimen was prepared by cutting in such a way that including the welded cross-section. And then, hardness scan was carried out along the cross-section of welded joint in Vickers scale at room temperature. The way of Vickers hardness scan and its result were shared in Figure 6. As a result of the hardness scans, it was observed that faying surface is harder through the weld zone as expected. Besides, the hardness values both on the faying surface and adjacent zone pointed out that the welding zone was suitable.

According to the weld zone hardness distribution seen in Figure 6b, the yield strength here corresponds to 940 MPa by converting the lowest hardness value to 300 HV to yield stress guided by ISO 18265 [24].

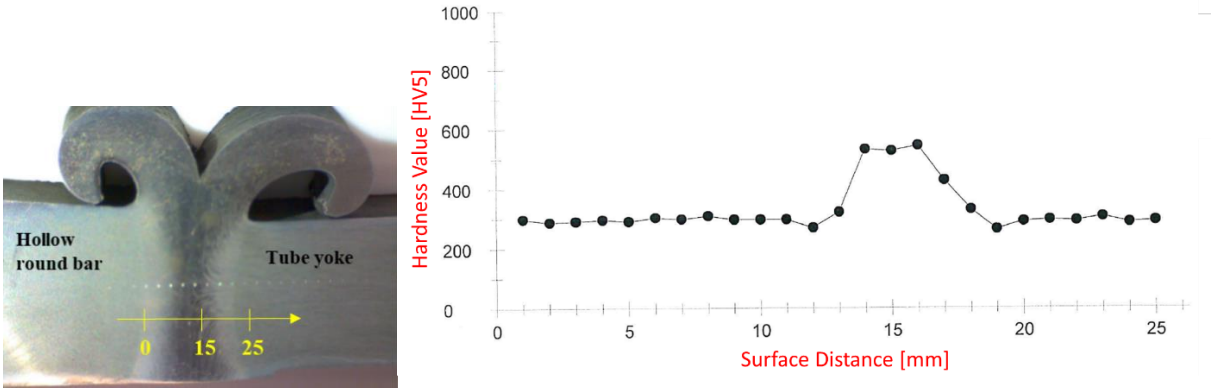

a) b)

Figure 6. Hardness scan of the cross-section of welded joint, a) hardness scan direction, b) hardness profile

Bending Test

The bending test was performed to investigate the joint quality and performance. And so, the joint area was inspected against possible linear discontinuity along the welding line.

The specimens were prepared in such a way of that covering the weld zone as having a size of 5x120 mm (thickness x length) from the cross-section of the welded joint. The specimen was supported with a vice, leaving the weld zone free to bend. Afterwards a force was applied to the free end of the specimen until it bended with 90 degrees. As seen in Fig. 7 no tearing was observed along the weld section.

a) b)

Figure 7. A bended specimen during the bending test to investigate the cross-section of welded joint in terms of the welding quality and performance.

Macroscopic/Microscopic Inspection

A specimen was cut from the welded yoke shaft for macro inspection. Respectively the specimen was polished and etched to reveal the weld and heat affected zone (HAZ). The specimen was taken under inspection to take macroscopic images. Macroscopic inspection of the longitudinal section of the welded joint showed us that there was no lack of fusion or cracking. Macrographs of the welded specimens were shown in Figure 8.

a) b)

Figure 8. A specimen under macroscopic inspections, a) welded yoke shaft, b) specimen sectioned from welded yoke shaft (Makroskopik incelemeler altındaki bir numune, a) kaynaklı çatallı mil, b) kaynaklı çatallı milden kesit numune).

Specimen for microscopic inspection were prepared by respectively sectioning, mounting, fine grinding, polishing, and etching (nital usage of 2%). Specimen was inspected with two separate magnifications as 10x and 50x. Microscopic inspection on the weld line of specimen revealed that there was no micro crack or any defects on the weld zone for both 10x and 50x magnification as in Figure 9.

a) b)

Figure 9. A specimen under microscopic inspections, a) 10x magnification on weld line, b) 50x magnification on weld line

After inspections, the welded yoke shafts were machined to reach the wall thickness defined in Table 2. And so, the final yoke shaft specimens were prepared in 3 groups; Group-1 doesn't involve any reduction of wall thickness while Group-2 and Group-3 involve. Driveshafts to be used in laboratory tests, an example of which is given in the Figure 10, were produced as 3 pieces for each group.

Table 2. The values of wall thickness of the specimens (Numunelerin et kalınlık değerleri)

Specimen ID	Wall Thickness A [mm]	
Group-1 (no reduction)	12	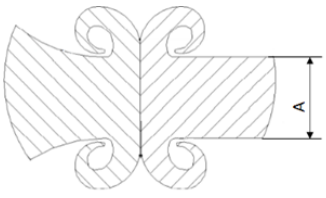
Group-2 (2 mm reduction)	10	
Group-3 (3 mm reduction)	9	

Figure 10. A drive shaft specimen produced for laboratory tests

2.2. Finite Element Analyses

Finite element analyses were applied on the 3D models which are prepared by considering the wall thicknesses reduced by machining the shank of welded yoke shaft. The yoke shaft 3D models designed with CatiaV5 R62020 computer aided design program was transferred to the HyperWorks-2021.2 computer aided finite element analysis program. For meshing, which is the first step of finite element analysis, necessary geometric arrangements were performed on the 3D model. Afterwards, a mesh structure on which the boundary conditions and external loads would be defined was established by using 3D tetra elements proper to size of the yoke shaft. The mesh structure was created by using the element size that has been proven by tests within the scope of one of our previous studies [25].

In the next step, two opposing yoke holes are connected to each other by rigid elements, and moment of 17.000 Nm is defined at the midpoint of the rigid member as in Fig. 11.

Like the yoke holes, the spline tooth faces are connected by rigid members and, assigned fixing elements to the midpoints of these rigid elements in such a way that there is no freedom in rotational and translational movements as in Fig. 11.

FEA models with the various wall thickness, which is prepared under the same conditions, was compared with each other. In addition, evaluating the models were not conducted by only FEA results but also laboratory testing. Considering all these, FEA model was prepared as one part due to the difficulty and uncertainty of the realization of the weld zone as a model.

The pre-processing for FEA were completed by defining respectively elasticity module and poison ratio as 210 GPa and 0.3. After these preparations analysis was carried out under structurally linear static condition.

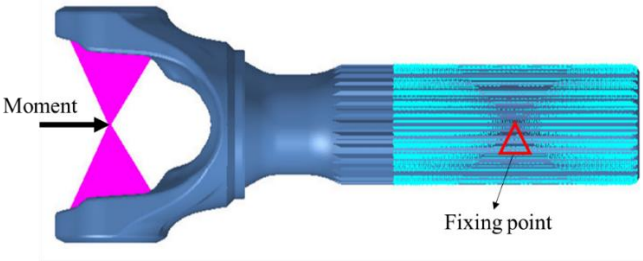

Figure 11. The FEA model after the pre-processing (Ön işlemeden sonraki FEA modeli)

2.3. Laboratory tests of the specimens

In the experimental studies, torsional tests were implemented on the drive shafts composed of welded yoke shafts produced by reducing the outer diameters of the welded components. Torsional tests were conducted for three groups of specimens, each containing two drive shafts, as defined in the Table 2. The test bench is specific for the drive shafts, and it is a custom production. The layout of the test bench was illustrated in the Figure 12. One end of the drive shaft was driven by the driven unit of the test machine while the other end of the drive shaft was fixed on the machine. The torque was applied in one direction defined in figure below.

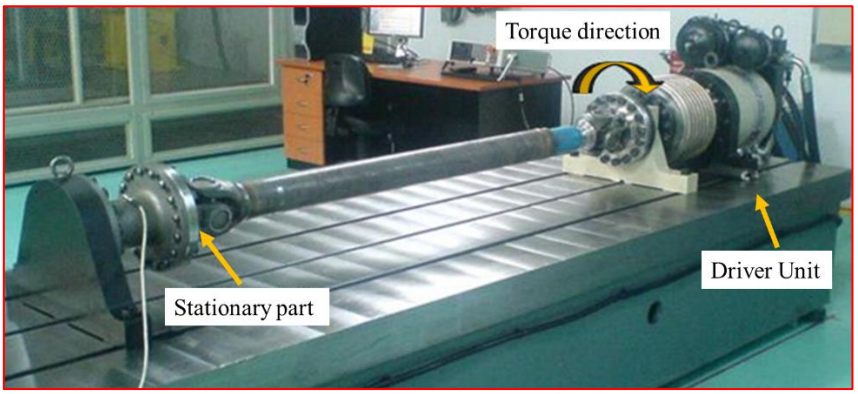

Figure 12. An illustration of the test bench (Test tezgahının bir örneği)

Each test was continued until any deformation was detected. Johnson's Apparent Elastic Limit (JAEL) values of the specimens were determined at the end of the tests.

3. EXPERIMENT AND OPTIMIZATION RESULTS (DENEY VE OPTİMİZASYON SONUÇLARI)

Johnson's Apparent Elastic Limit (JAEL) values of the specimens were determined at the end of the tests as given in Table 3. JEAL values of the specimens are compliant with the wall thickness, as expected. So, JEAL decreases as the wall thickness decreases.

Von Mises stress values on the shank, which are obtained from FEA, have been taken into consideration for comparison of three Group of specimens and they were listed in Figure 13. The stress values on the spline, which is in red, has been ignored because they occur due to lack of freedom.

The values of the hardness scan were considered to evaluate the stress obtained by FEA, which is corresponding to the weld zone.

Table 3. Torsional test results

Specimen ID	Wall Thickness [mm]	JAEL [kNm]	
Group-1	12	18.0	19.4
Group-2	10	17.5	17.1
Group-3	9	17.0	17.3

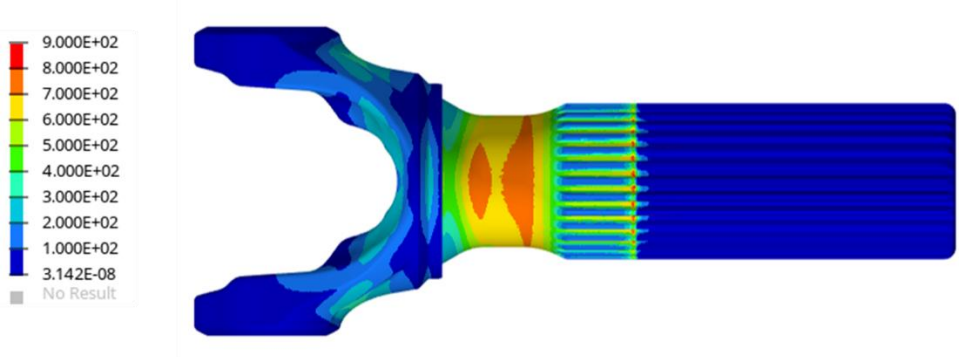

Specimen ID	Wall Thickness on Shank [mm]	Stress on Shank [MPa]
Group-1	12	606
Group-2	10	695
Group-3	9	763

Figure 13. FEA results for three group of specimens

4. CONCLUSIONS (SONUÇLAR)

In the study, tube yoke and hollow yoke bar were joined successfully by using CDFW method. Welded yoke shafts were subjected to consecutive machining processes to reduce the wall thickness. Finally, the effect of reduced shank thickness of friction welded yoke shaft on strength was investigated by FEA and laboratory tests. Important outputs of the study are as follows:

1. While the yield strength for tube yoke material is 820 MPa, it is 700 MPa for hollow round bar material. The yield strength of the weld zone obtained as 940 MPa by converting the lowest hardness value (300 HV) to yield stress guided by ISO 18265.
2. It is possible to use the product with reduced wall thickness which is obtained in a way of removing material from the outer surface of the shank as long as the machined product serves for the desired torque capacity.
3. Product with 9 mm wall thickness of shank, which is obtained after machining operation of product with 12 mm wall thickness of shank, produced by rotary friction welding method, can be used instead of product with 12 mm of wall thickness when considered the desired torque capacity of 17 kNm.
4. A comprehensive study is required to realize the friction weld zone in finite element analysis. Because uncertainties and difficulties prevail in friction welding modelling.

ACKNOWLEDGMENTS (TEŞEKKÜR)

This study was carried out with the facilities and support of Tirsan Kardan A.Ş. R&D Center.

REFERENCES (KAYNAKLAR)

1. S.W. Kallee, E.D. Nicholas, M.J. Russell, Friction welding of aero engine components, 10th World Conference on Titanium Ti-2003, 2003, Hamburg, Germany.
2. V. I. Vill, Friction Welding of Metals, American Welding Society, New York, 1962.
3. W. Kinley, Inertia welding: simple in principle and application, Welding and Metal Fabrication, 585–589, 1979.
4. N. Fomichev, The friction welding of new high-speed tool steels to structural steels, Weld Prod, 27(4): 31-34, 1980.
5. M. Maalekian, Friction welding critical assessment of literature, Science and Technology of Welding and Joining, 12(8): 738-759, 2007.
6. ANSI/AWS C6.1-89, Recommended Practices for Friction Welding, American National Standards Institute, 1989.
7. T. Lienert, W.A. Baeslack, J. Ringnalda, H.L. Fraser, Inertia-friction welding of SiC-reinforced 8009 aluminium, J Mater Sci, 31(8): 2149–2157, 1996.
8. V.V. Satyanarayana, G.M. Reddy, T.J. Mohandas, Dissimilar metal friction welding of austenitic–ferritic stainless steels, Journal of Materials Processing Technology, 160: 128–137, 2005.
9. A. Ambroziak, Friction welding of titanium–tungsten pseudoalloy joints, Journal of Alloys and Compounds, 506(2): 761–765, 2010.
10. H.C. Dey, M. Ashfaq, A.K. Bhaduri, K.R. Prasad, Joining of titanium to 304L stainless steel by friction welding, Journal of Materials Processing Technology, 209(18-19):5862–5870, 2009.
11. G.J. Bendzsak, T.H. North, Z. Li, Numerical model for steady-state flow in friction welding, Acta Materialia, 45(4): 1735–1745, 1997.
12. M. Kimura, M. Kusaka, K. Seo, A. Fuji, Improving Joint Properties of Friction Welded Joint of High Tensile Steel, JSME Int J Ser A, 48(4): 399–405, 2005.
13. Z.W. Huang, H.Y.Li, M. Preuss, M. Karadge, P. Bowen, S. Bray, G. Baxter, Inertia friction welding dissimilar nickel-based superalloys alloy 720Li to IN718, Metallurgical and Materials Transactions A, 38(7): 1608-1620, 2007.
14. W.B. Lee, M.G. Kim, J.M. Koo, K.K. Kim, D.J. Quesnel, Y.J. Kim, S.B. Jung, Friction welding of TiAl and AISI4140, Journal of Materials Science, 39(3):1125–1128, 2004.
15. P. Sathiya, S. Aravindan, A.N. Haq, Some experimental investigations on friction welded stainless steel joints, Materials & Design, 29(6): 1099-1109, 2008.
16. B. Uday, M. N. Ahmad Fauzi, H. Zuhailawat i, A. B. Ismail, Advances in friction welding process: A review, Science and Technology of Welding and Joining, 15(7): 534-558, 2010.

17. İ. Çelikyürek, O. Torun, B. Baksan, Microstructure and strength of friction-welded Fe-28Al and 316 L stainless steel, Materials Science and Engineering: A, 528(29): 8530-8536, 2011.
18. M. Maalekian, Thermal modelling of friction welding, ISIJ International, 10: 1429–1433, 2008.
19. O.T. Midling, Ø. Grong, A process model for friction welding of Al-Mg-Si alloys and Al-SiC metal matrix composites, Acta Metallurgica et Materialia, 42(5): 1595-1622, 1994.
20. M. Kimura, M. Kusaka, K. Kaizu, et al., Friction welding technique and joint properties of thin-walled pipe friction-welded joint between type 6063 aluminum alloy and AISI 304 austenitic stainless steel, Int J Adv Manuf Technol 82: 489–499, 2016.
21. M.B. Uday, M.N. Ahmad Fauzi, H. Zuhailawati, A.B. Ismail, Effect of welding speed on mechanical strength of friction welded joint of YSZ–alumina composite and 6061 aluminum alloy. Materials Science and Engineering: A, 528(13–14): 4753-4760, 2011.
22. E. P. Alves, F. P. Neto, C.Y. An., Welding of AA1050 aluminum with AISI 304 stainless steel by rotary friction welding process, Journal of Aerospace Technology and Management, 2(3): 301-306, 2010.
23. J.T. Xiong, J.L. Li, Y.N. Wei, F.S. Zhang, W.D. Huang, An analytical model of steady-state continuous drive friction welding, Acta Materialia, 61(5): 1662-1675, 2013.
24. ISO 18265:2013, Metallic materials-Conversion of hardness values, International Organization for Standardization, 2013.
25. O. Şen, M.C. Kahyalar, Structural analysis of yoke part in design of driveshaft, International Journal Of Automotive Science and Technology, 4(4): 248-252, 2020.